


RESEARCH ARTICLE

Adrenal-Specific KO of the Circadian Clock Protein BMAL1 Alters Blood Pressure Rhythm and Timing of Eating Behavior

Hannah M. Costello^{1,2,3}, G. Ryan Crislip^{1,2,3}, Kit-Yan Cheng^{1,2},
I. Jeanette Lynch^{2,4}, Alexandria Juffre^{1,2,5}, Phillip Bratanatawira²,
Annalisse Mckee¹, Ryanne S. Thelwell¹, Victor M. Mendez¹,
Charles S. Wingo^{2,4}, Lauren G. Douma^{1,2,3}, Michelle L. Gumz ^{1,2,3,4,5,*}

¹Department of Physiology and Aging, University of Florida, Gainesville, FL 32610, USA, ²Department of Medicine, Division of Nephrology, Hypertension, and Renal Transplantation, University of Florida, Gainesville, FL 32610, USA, ³Center for Integrative Cardiovascular and Metabolic Diseases, University of Florida, Gainesville, FL 32610, USA, ⁴Research, North Florida/South Georgia Malcolm Randall Veterans Affairs Medical Center, Gainesville, FL 32608, USA and ⁵Department of Biochemistry and Molecular Biology, University of Florida, Gainesville, FL 32610, USA

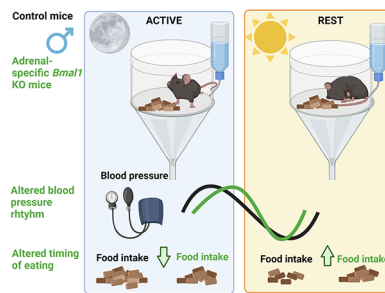
*Address correspondence to M.L.G. (e-mail: Michelle.Gumz@medicine.ufl.edu)

Abstract

Brain and muscle ARNT-like 1 (BMAL1) is a core circadian clock protein and transcription factor that regulates many physiological functions, including blood pressure (BP). Male global *Bmal1* knockout (KO) mice exhibit ~10 mmHg reduction in BP, as well as a blunting of BP rhythm. The mechanisms of how BMAL1 regulates BP remains unclear. The adrenal gland synthesizes hormones, including glucocorticoids and mineralocorticoids, that influence BP rhythm. To determine the role of adrenal BMAL1 on BP regulation, adrenal-specific *Bmal1* (*AS^{Cre/+}::Bmal1*) KO mice were generated using aldosterone synthase Cre recombinase to KO *Bmal1* in the adrenal gland zona glomerulosa. We confirmed the localization and efficacy of the KO of BMAL1 to the zona glomerulosa. Male *AS^{Cre/+}::Bmal1* KO mice displayed a shortened BP and activity period/circadian cycle (typically 24 h) by ~1 h and delayed peak of BP and activity by ~2 and 3 h, respectively, compared with littermate Cre- control mice. This difference was only evident when KO mice were in metabolic cages, which acted as a stressor, as serum corticosterone was increased in metabolic cages compared with home cages. *AS^{Cre/+}::Bmal1* KO mice also displayed altered diurnal variation in serum corticosterone. Furthermore, these mice have altered eating behaviors where they have a blunted night/day ratio of food intake, but no change in overall food consumed compared with controls. Overall, these data suggest that adrenal BMAL1 has a role in the regulation of BP rhythm and eating behaviors.

Submitted: 19 November 2022; Revised: 16 December 2022; Accepted: 17 December 2022

© The Author(s) 2023. Published by Oxford University Press on behalf of American Physiological Society. This is an Open Access article distributed under the terms of the Creative Commons Attribution-NonCommercial License (<https://creativecommons.org/licenses/by-nc/4.0/>), which permits non-commercial re-use, distribution, and reproduction in any medium, provided the original work is properly cited. For commercial re-use, please contact journals.permissions@oup.com



Key words: Blood pressure; brain and muscle ARNT-like 1; circadian rhythms; adrenal gland; feeding; corticosterone

Introduction

Blood pressure (BP) exhibits a circadian rhythm, characterized by a morning surge on waking and a 10%–20% decline or dip in pressure during the rest period. Loss of this rhythm is associated with adverse cardiorenal outcomes.¹ Furthermore, circadian disruption, defined as misalignment between endogenous circadian rhythms and behavioral rhythms, can be experienced by individuals undergoing shiftwork, or chronic jet lag. This misalignment is also associated with worsened health outcomes, including hypertension.^{2,3} Importantly, a delay or advance of just one hour is associated with increased adverse cardiovascular events as well as increased traffic accidents,^{4,5} underscoring the critical role of precise timing in maintaining health. Understanding the molecular mechanisms of how these rhythms are regulated and its implications for health is needed as hypertension is the leading modifiable risk factor for all-cause mortality.^{6,7} With humans and mice having comparable rhythms, albeit inverted due to diurnal and nocturnal behaviors, respectively,⁸ mouse models are useful tools to study the mechanisms by which circadian rhythms contribute to the regulation of physiological function.

Circadian rhythms are regulated in part by the central circadian clock, which resides in the suprachiasmatic nucleus (SCN) of the hypothalamus, and peripheral clocks throughout the body. It is widely accepted that the central clock is entrained by light cues, and acts as a pacemaker to synchronize peripheral clocks. More recently, timing of food intake has been shown to be an important zeitgeber (external timing cue) for synchronization of peripheral clocks.^{9–12} At the molecular level, the circadian clock is present in nearly every cell type and consists of a series of transcriptional, translational, and post-translational feedback loops, for more details see.¹³ More simply, at the core of the clock mechanism, four transcription factor proteins, Brain and muscle aryl hydrocarbon receptor nuclear translocator (ARNT)-like protein (BMAL1), CLOCK, Cryptochrome (CRY), and Period (PER), function to regulate gene expression in a tissue-specific manner. BMAL1 and CLOCK are part of the positive arm of the clock machinery, which form a heterodimer and bind to enhancer box (E-Box) promoter response elements to enhance the transcription of target genes. Target genes include *Cry* and *Per*, which encode the proteins CRY and PER that act in the negative arm to inhibit the actions of BMAL1 and CLOCK.^{14,15}

Our laboratory and others have utilized mouse models knocking out BMAL1 to explore the role of BMAL1 in BP regulation. Curtis et al. showed that global *Bmal1* knockout (KO) male mice exhibit ~10 mmHg reduction in BP, as well as a blunting of the BP rhythm.¹⁶ Xie et al. showed a reduction in BP in smooth muscle *Bmal1* KO male mice, with less disruption of BP rhythm than in the global KO.¹⁷ With the kidney playing an

important role in BP,¹⁸ kidney-specific *Bmal1* KO mice have been generated, including an inducible tubule-specific KO,¹⁹ collecting duct-specific KO,²⁰ distal nephron and collecting duct KO,²¹ and renin cell-specific KO.²² All these models exhibited lower BP in male mice, although BP rhythm remained intact, suggesting a critical role for BMAL1 in BP regulation, independent of rhythm. To date, no tissue-specific *Bmal1* KO models studied have fully recapitulated the global KO phenotype, therefore raising the question of what other tissues contribute to the blunting of BP rhythm in the global *Bmal1* KO male mice?

The adrenal gland synthesizes hormones, including cortisol (corticosterone in rodents) and aldosterone, and these hormones exert a powerful influence on BP rhythm.²³ Interestingly, adrenal-specific *Bmal1* KO male and female mice showed augmented plasma corticosterone following an acute restraint stressor.²⁴ However, the role of the adrenal clock in the regulation of BP remains unknown.

In the present study, we used adrenal-specific aldosterone synthase ($AS^{Cre/+}$, $Cyp11b2^{tm1.1(cre)Brlt}$) Cre recombinase to generate adrenal-specific *Bmal1* ($AS^{Cre/+}::Bmal1^{FL/FL}$) KO mice to test the hypothesis that adrenal BMAL1 is required for BP regulation and normal circadian rhythms of BP in male mice. Limited studies have been performed in female *Bmal1* KO models, but given that female kidney-specific *Bmal1* KO mice did not exhibit a change in BP or any BP rhythm changes,^{20,21} this study focused on male $AS^{Cre/+}::Bmal1$ KO mice.

Materials and Methods

Animals

The mouse model used in this study was generated using floxed exon 8 *Bmal1*^{FL/FL} mice [a gift from Dr. Karyn Esser, University of Florida¹⁷] crossed with adrenal-specific aldosterone synthase ($AS^{Cre/+}$, $Cyp11b2^{tm1.1(cre)Brlt}$) Cre recombinase mice [obtained from Dr. David Breault, Harvard^{24–26}], generating $AS^{Cre/+}::Bmal1$ KO mice. The original $AS^{Cre/+}$, $Cyp11b2^{tm1.1(cre)Brlt}$ mice were on a mixed C57BL/6 J/129sv background. In our hands, Transnetyx SNP analysis from representative mice showed that the genetic background was $97.13\% \pm 0.41\%$ C57BL/6 J following backcrossing to ~C57BL/6 J for 8 generations at the University of Florida. Mice (16–20 wk) were housed on a 12-h light/12-h dark cycle, with lights on at 6 AM [zeitgeber time (ZT)0] and lights off at 6 PM (ZT12). Mice were provided *ad libitum* access to the control diet (0.25% NaCl, 0.6% K; carbohydrate 58.7% by weight, protein 18.3% by weight, and fat 7.2% by weight; Envigo Teklad custom diet TD.99131) and water. All experiments involving animals were approved by the University of Florida and the North Florida/South Georgia Veterans Administration Institutional Animal Care and Use Committees (IACUC) in accordance

with the National Institutes of Health Guide for the Care and Use of Laboratory Animals.

Recombination PCR

Genomic DNA was extracted from adrenal glands using three different primers for recombination triplex PCR [forward primer (5'-ACTGGAAGTAACTTTATCAAAGT-3'), loxP reverse primer (5'-CTGACCAACTTGCTAACAATTA-3'), and recombination reverse primer (5'-CTCCTAACTTGGTTTTGTCTGT-3')] to detect the successful recombination and subsequent deletion of exon 8 of BMAL1 following Cre recombinase-mediated excision in AS^{Cre/+}::Bmal1 KO mice and AS^{+/+}::Bmal1^{Fl/Fl} Cre- littermate control mice.²¹ Other tissues were assessed, including the kidney, heart, aorta, liver, lung, brain, and testes to determine if KO was specific to the adrenal gland.

Immunohistochemistry

Adrenal glands were collected at 10 AM and fixed with periodate-lysine-2% paraformaldehyde to assess the efficacy of BMAL1 KO, using immunohistochemistry (IHC) as described in.²¹ In brief, adrenal glands were embedded in polyester wax, and 5 μm thick sections were cut and mounted on glass slides. Sections were dewaxed in ethanol, rehydrated, incubated in heated Trilogy Antigen Retrieval (Cell Marque), then 3% H₂O₂ to block endogenous peroxidase activity. Dako protein blocker was used before being incubated overnight at 4 degrees with BMAL1 primary antibody (Cell Signaling). Sections were incubated with secondary antibody (Vector ImmPress Rabbit Ig) for 30 min then 3,3'-diaminobenzidine chromogenic substrate for detection (Vector). Finally, sections were washed, dehydrated, and mounted. Three nonoverlapping representative images of each adrenal gland region (zona glomerulosa, zona fasciculata, and medulla) were taken at x40 magnification (Nikon E600 equipped with a Nikon DXM1200F digital camera). IHC images were analyzed using ImageJ.

Radiotelemetry and Metabolic Cages

Radiotelemetry devices (Data Science International) were implanted into the carotid artery and extended into the aortic arch of 16-wk-old AS^{Cre/+}::Bmal1 KO male mice and littermate controls, previously described in.^{27,28} After 7–10 d of recovery, telemetry recordings were made for three consecutive days in home cages to measure mean arterial pressure (MAP), heart rate (HR), and locomotor activity. Mice were then placed in metabolic cages to acclimate for 3 d. MAP, HR, and locomotor activity were then recorded for three consecutive days. Twelve-hour food and water intake, and 12-h urine output were measured during this period, with food dishes replaced daily at 6 AM.

Cosinor Analysis

With BP, HR, and activity being rhythmic, cosinor analysis is used to calculate the period, the midline estimating statistic of rhythm (MESOR), amplitude, acrophase, and robustness. The period is the time taken for a full cycle, or from one peak of an oscillation to the next. MESOR is an estimate of central tendency as it takes circadian rhythm into account. Amplitude is the difference between the peak of a rhythm and the MESOR. Acrophase is the time at which the peak of a rhythm occurs. Robustness is the strength of the rhythm and is calculated as the percentage of variance accounted for by the Cosinor model.²¹

Analysis was performed on each mouse separately over the 3 d in the home cage and metabolic cage using Cosinor software designed by,²⁹ and presented as the mean ± SD for each genotype. Rayleigh plots were generated and statistical tests performed using Oriana software.³⁰

Flame Photometry

Flame photometry (model 2655-00, Cole-Parmer) was used to determine urine sodium and potassium concentrations.^{21,31}

Aldosterone ELISA

Urinary aldosterone was quantified using an aldosterone ELISA kit (Enzo, ADI-900-173), according to the manufacturer's instructions. The cross-reactivity for this kit is 100% for aldosterone, 0.3% 11-deoxycorticosterone, 0.19% corticosterone, 0.2% progesterone, and < 0.001% for cortisol, dihydrotestosterone, estradiol, and testosterone. The detectable range is from 3.9–250 pg/mL.³¹

Corticosterone ELISA

In a separate cohort of mice, serum was collected by the tail nick technique at 6 AM (lights on) and 6 PM (lights off). Blood (~20 μL) was collected within 1 min of disturbing either the mouse's home or following in metabolic cages and while minimally restrained to acquire home or metabolic cage corticosterone measurements. Measurements were first completed in home cages, and measurements were repeated in the same animal following 5 d in metabolic cages. Serum corticosterone concentration was quantified using a corticosterone ELISA kit (Enzo, ADI-900-097), according to manufacturer's instructions. The cross-reactivity for this kit is 100% for corticosterone, 21.3% 11-deoxycorticosterone, 21.0% desoxycorticosterone, 0.46% progesterone, 0.31% testosterone, 0.28% tetrahydrocorticosterone, 0.18% aldosterone, 0.046% cortisol, and < 0.03% for pregnenolone, estradiol, cortisone, and 11-dehydrocorticosterone acetate. The detectable range is from 32–20 000 pg/mL.

Statistics

Graphpad Prism was used to perform t-tests, 2-way ANOVA with repeated measures, and 3-way ANOVA with repeated measures to determine effect of time (ZTO, ZT12) and/or cage and genotype with Šidák multiple comparisons *post hoc* analysis. All values are presented as mean ± SD.

Results

Verification of AS^{Cre/+}::Bmal1 KO Model

To confirm the localization and efficacy of the KO of adrenal-specific BMAL1, recombination PCR and IHC were performed. Recombination PCR yielded a smaller 430-bp band, encompassing a loxP site in the intact floxed *Bmal1* gene present in tissues not expressing AS-Cre recombinase, including in the adrenal gland of floxed *Bmal1* Cre- littermate control mice (Figure 1A and B). It also yielded a 570-bp band only present in the adrenal glands of AS^{Cre/+}::Bmal1 KO mice (denoted by * in Figure 1B) due to recombination and deletion of the sequence between the loxP sites by Cre recombinase. The adrenal glands of AS^{Cre/+}::Bmal1 KO mice also yielded the smaller band as aldosterone synthase is not present in all cells of the adrenal gland. There was no evidence of recombination in other tissues (kidney, heart, aorta,

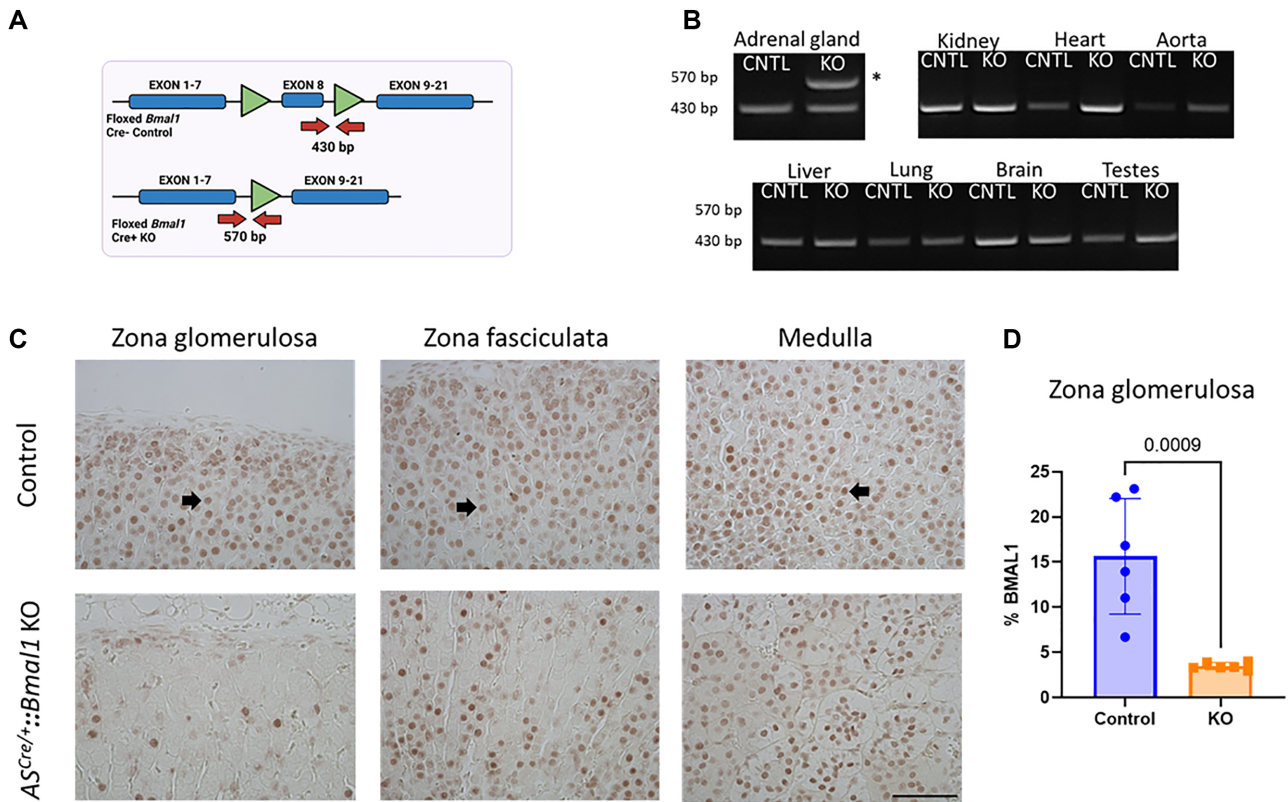


Figure 1. Verification of the $AS^{Cre/+};Bmal1$ KO model. **A.** Schematic diagram shows the placement of loxP sites flanking exon 8 on the *Bmal1* gene and the location of primers (red arrows; forward, loxP reverse, and recombination primers) used in recombination PCR to measure the specificity of *Bmal1* KO by aldosterone synthase Cre. Band product of 570-bp yielded from recombined floxed *Bmal1* Cre + KO gene. **B.** Recombination PCR showing expected 570-bp product in adrenal glands of $AS^{Cre/+};Bmal1$ KO mice, with lack of this product in kidney, heart, aorta, liver, lung, brain, and testes of control and $AS^{Cre/+};Bmal1$ KO mice confirming that recombination is only detected in the adrenal gland of $AS^{Cre/+};Bmal1$ KO mice (CNTL, control mice; KO, $AS^{Cre/+};Bmal1$ KO mice). Images are representative of $n = 4$ per genotype and sex. **C.** Representative immunohistochemical images of BMAL1 protein expression in zones of the adrenal gland of control or $AS^{Cre/+};Bmal1$ KO male mice. Black arrows indicate BMAL1-positive stained nuclei. Images were taken at 40x magnification and the scale bar = 0.05 mm. **D.** Quantification of % BMAL1 from control (blue circles) and KO (orange squares) adrenal glands was performed using ImageJ ($n = 6$ mice per genotype). Values are means \pm SD. Student's *t*-test was used to compare genotypes.

liver, lung, brain, and testes (Figure 1B). Figure 1C shows BMAL1 protein expression in the zones of the adrenal gland of control and KO mice, using IHC, showing > 75% reduction of BMAL1 in the zona glomerulosa ($P = 0.0009$, Figure 1D).

$AS^{Cre/+};Bmal1$ KO Mice Display Shifted Acrophase of BP and Activity in Metabolic Cages

We performed a radiotelemetry study to determine the contribution of adrenal BMAL1 on BP, HR, and activity. There were significant time effects with no significant genotype effects in the 1-h averages over 3 d for MAP, HR, and activity in home cages (Figure 2A–C). To note, basal MAP was higher in both KO and littermate control mice than reported C57BL/6 wild-type mice³² but similar to previously reported 129/sv male mice.^{28,33} There were no BMAL1-dependent changes in the 1-h averages over 3 d for MAP, HR, and activity following placement in metabolic cages (Figure 2D–F). There was a significant interaction between genotype and time in both MAP and HR, with activity not reaching significance ($P = 0.1045$). Furthermore, averaged 24-h MAP, HR, and activity were calculated (Figure 2G–I), showing a significant cage effect in MAP and HR, but not activity. Thus, we performed cosinor analysis on data from parameters measured in both

home and metabolic cages, which revealed significant genotype differences in BP rhythm only in metabolic cages (Table 1). The period (time taken for a full circadian cycle, typically 24 h) was significantly shortened for MAP in $AS^{Cre/+};Bmal1$ KO mice compared with littermate control mice in metabolic cages (MAP 23 h 30 vs 24 h 18, $P = 0.01$). Furthermore, the acrophase (the time at which the peak of BP occurs) was shifted ~ 2 h later in KO mice in metabolic cages (KO ZT17 h 38 vs control ZT15 h 45, $P = 0.002$). The MESOR, amplitude (difference between peak and MESOR), and robustness (strength of the rhythm) of MAP remained similar between groups. For activity, the period was also shortened (KO 23 h 18 vs control 24 h 54, $P = 0.0033$) and the acrophase delayed ~ 3 h (KO ZT16 h 46 vs control ZT13 h 59, $P = 0.0017$). The acrophase was further evaluated by a Rayleigh plot, in which data are represented on a 24-h clock.²⁹ Each data point represents the time of the peak of the rhythm, and the distance of each data point from the center corresponds to the amplitude. Acrophase for both MAP and activity in $AS^{Cre/+};Bmal1$ KO mice were clustered together so remained synchronized, albeit delayed relative to control mice (Figure 3). Comparisons in cosinor parameters between home and metabolic cages within each genotype highlighted the effect of metabolic cages on MAP and HR rhythm, where MESOR was significantly increased, and both amplitude and robustness reduced, regardless of

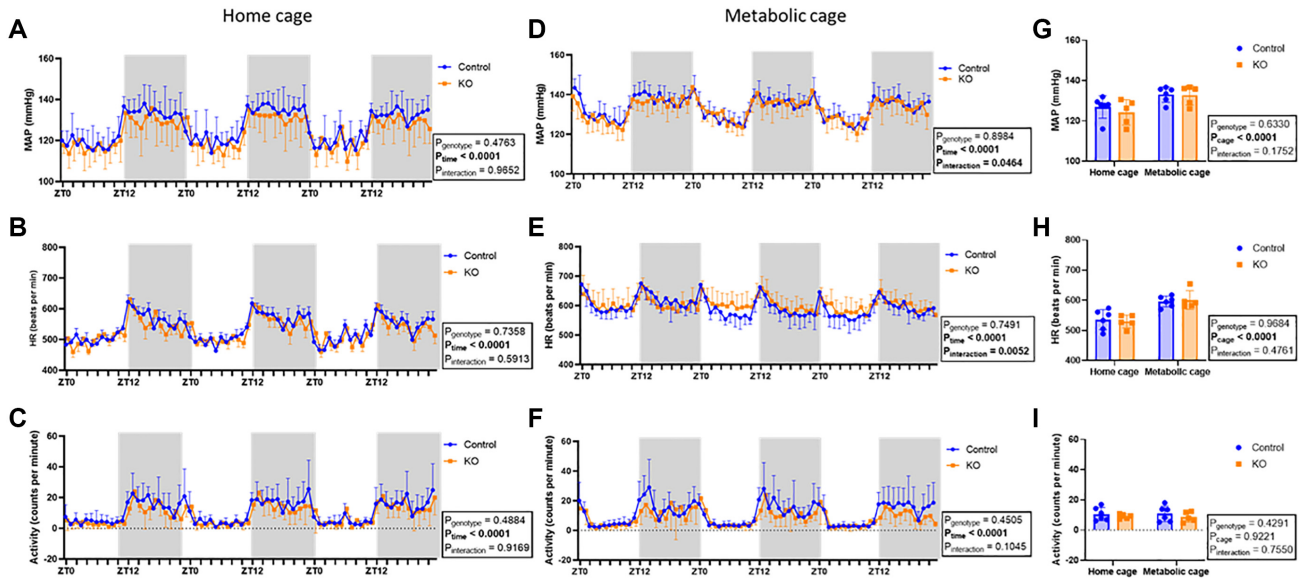


Figure 2. AS^{Cre/+}::Bmal1 KO mice exhibit altered MAP and HR, but not activity in response to placement in metabolic cages. Hourly averages in ZT over 72 h of MAP, HR, and activity in home cages (A–C) and metabolic cages (D–F) in control (blue circles, n = 6) and AS^{Cre/+}::Bmal1 KO (orange squares, n = 5) male mice. ZT0 represents lights on and ZT12 represents lights off. The shaded background indicates the active period (lights off, night). Averaged 24-h MAP (G), HR (H), and activity (I) in homes and metabolic cages. Values are expressed as means ± SD. Genotype, cage, and interaction effects were determined by a 2-way ANOVA with repeated measures.

Table 1. Cosinor Analysis of MAP, HR, and Activity Measured via Telemetry from Male Mice in Home Cages vs Metabolic Cages

	Home Cage			Metabolic Cage		
	Control	AS ^{Cre/+} ::Bmal1 KO	P value	Control	AS ^{Cre/+} ::Bmal1 KO	P value
	Mean arterial pressure			Mean arterial pressure		
Period (h)	23h59 ± 0h13	23 h 45 ± 0 h 49	0.5440	24h18 ± 0h24	23 h 30 ± 0 h 18 [†]	0.0195*
MESOR (counts per min)	126.6 ± 5.0	122.7 ± 5.6	0.4792	133.5 ± 3.5 [†]	132.7 ± 4.4 [†]	0.9035
Amplitude (counts per min)	9.1 ± 0.9	7.5 ± 2.4	0.3982	4.9 ± 0.5 [†]	5.2 ± 0.9 [†]	0.8604
Acrophase (h)	ZT15h19 ± 0h20	ZT15h40 ± 0h49	0.7901	ZT15h45 ± 0h23	ZT17h38 ± 0h49 [†]	0.0021*
Robustness (%)	87.7 ± 8.6	80.6 ± 10.3	0.6309	62.2 ± 6.9 [†]	66.5 ± 13.3 [†]	0.8062
	Heart rate			Heart rate		
Period (h)	24h00 ± 0h37	23h35 ± 0h26	0.8288	23h42 ± 1h24	23h12 ± 2h00	0.6471
MESOR (counts per min)	535.9 ± 30.7	525.0 ± 19.1	0.7400	594.9 ± 17.1 [†]	599.6 ± 26.5 [†]	0.7496
Amplitude (counts per min)	43.1 ± 12.9	31.8 ± 12.7	0.4872	16.3 ± 5.8 [†]	14.1 ± 7.1 [†]	0.3763
Acrophase (h)	ZT13h38 ± 0h53	ZT13h59 ± 0h53	0.7882	ZT13h04 ± 3h43	ZT08h35 ± 5h03	0.1383
Robustness (%)	77.1 ± 8.5	60.0 ± 15.9	0.2602	21.9 ± 10.3 [†]	26.9 ± 16.2 [†]	0.8117
	Activity			Activity		
Period (h)	24h14 ± 0h11	24h06 ± 0h14	0.1589	24h54 ± 0h48	23h18 ± 0h24 [†]	0.0033*
MESOR (counts per min)	9.2 ± 4.0	9.1 ± 1.4	0.5142	9.3 ± 4.8	8.6 ± 3.0	0.4418
Amplitude (counts per min)	6.1 ± 2.8	6.4 ± 1.7	0.6033	5.3 ± 3.9	4.9 ± 2.2	0.4496
Acrophase (h)	ZT14h53 ± 0h34	ZT14h54 ± 0h34	0.9702	ZT13h 59 ± 0h38	ZT16h46 ± 1h14 [†]	0.0017*
Robustness (%)	76.7 ± 9.7	73.5 ± 17.5	0.5768	54.8 ± 12.3 [†]	58.6 ± 10.2 [†]	0.8954

Values are expressed as means ± SD (n = 5–6). The period, MESOR, amplitude, acrophase, and robustness were calculated for MAP, HR, and activity from AS^{Cre/+}::Bmal1 KO and control male mice in home cages and metabolic cages. Student’s t-test was used for comparisons with p values expressed for comparisons between genotypes within each cage.

*Significant comparison between genotypes within each cage.

[†]Significant comparison between cages within each genotype.

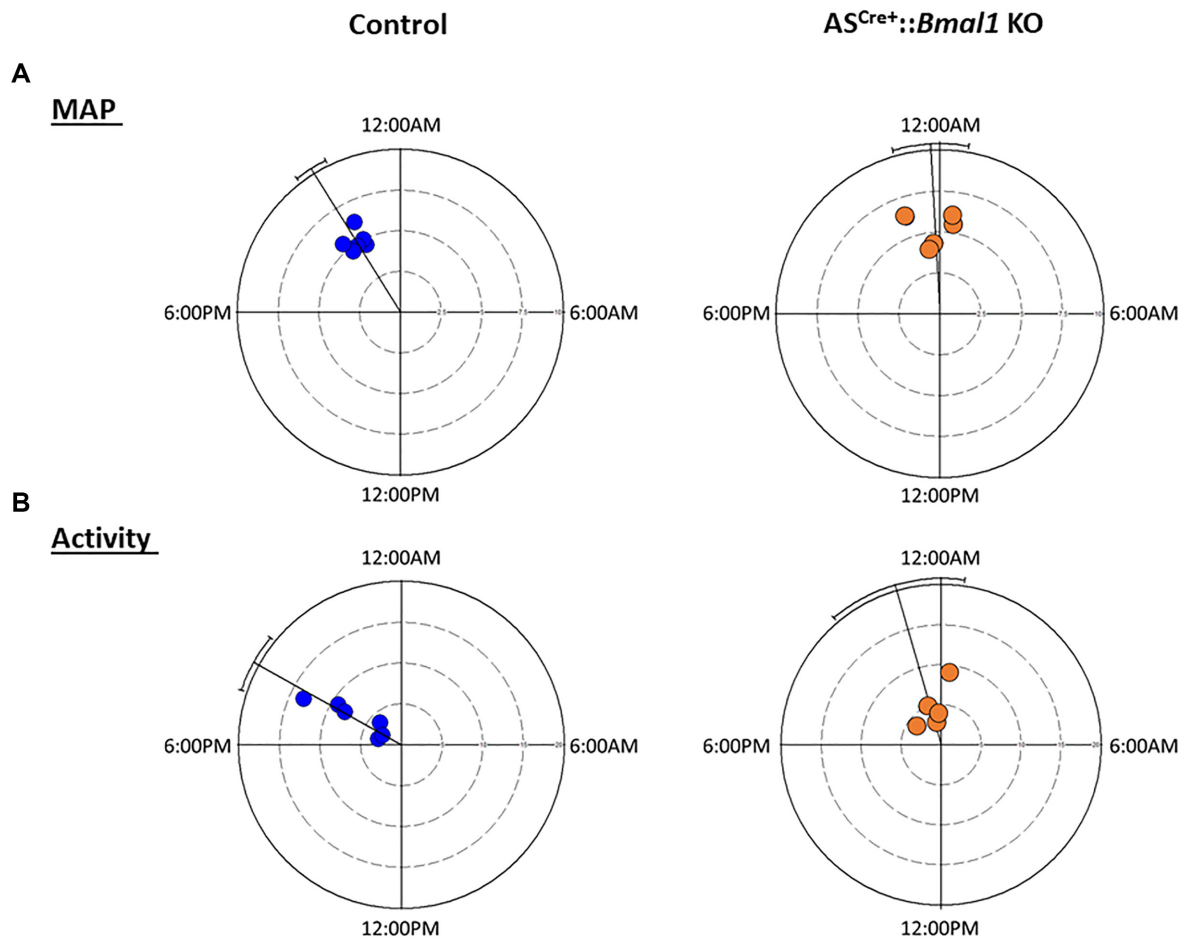


Figure 3. *AS^{Cre/+};;Bmal1 KO* mice display a delayed peak of BP and activity in metabolic cages. Rayleigh plots showing the acrophase on a 24-h clock where each data point represents the time of the peak of the MAP (A) or activity (B) rhythm in control (blue circles, $n = 6$) and *AS^{Cre/+};;Bmal1 KO* (orange squares, $n = 5$) male mice. The distance of each data point from the origin corresponds to the amplitude. Values are expressed as the mean acrophase over a 72-h period and error bars are SD.

genotype (Table 1). For activity, robustness was reduced following placement in metabolic cages and this effect was independent of genotype. In contrast, the period was significantly shorter and the acrophase significantly delayed for MAP and activity in *AS^{Cre/+};;Bmal1 KO* mice in metabolic cages compared to home cages. These effects suggest that changes in BP and activity rhythm in response to placement in metabolic cages are BMAL1-dependent.

AS^{Cre/+};;Bmal1 KO Alters Night/Day Ratio of Eating Behavior, Influencing Timing of Sodium, and Potassium Balance

The advantage of placing the mice in metabolic cages is that accurate food and water intake and urine output can be measured. Average 24-h food intake was not significantly different between genotypes (Figure 4A). Day and night food intake were assessed and demonstrated a significant interaction between genotype and time ($P = 0.0058$; Figure 4B). This led us to calculate the night/day ratio of food intake, which was significantly reduced in *AS^{Cre/+};;Bmal1 KO* mice compared with controls ($P = 0.0008$, Figure 4C). Water intake (24-h total, 12-h or night/day ratio) was not different between genotypes (Figure 4D–F). Urine output was similar over 3 d on the control diet in control and KO animals (Figure 5A). Sodium and potassium excretion were averaged over the 3 d and displayed significant time effects but were

similar between genotypes (Figure 5B and D). Sodium and potassium balances were calculated by subtracting urinary excretion from dietary intake. There was a significant interaction between genotype and time for sodium balance ($P = 0.0189$; Figure 5C) and for potassium balance ($P = 0.0336$; Figure 5E), both of which appeared more positive during the day (rest phase) and more negative during the night (active phase) in KO vs control. Lastly, urinary aldosterone, an adrenal hormone known to regulate sodium and potassium balance, was measured. As expected, active-phase aldosterone excretion was higher than daytime ($P < 0.0001$) without an apparent effect of genotype ($P = 0.1387$; Figure 5F).

Serum Corticosterone in Home and Metabolic Cages in *AS^{Cre/+};;Bmal1 KO* Mice

With metabolic cage telemetry data suggesting that mice were under stress, the effect of placing mice into metabolic cages on serum corticosterone was assessed to determine the effects of time-of-day, genotype, and cage. Three-way ANOVA demonstrated significant effects of time and cage on serum corticosterone (Figure 6). Furthermore, there was a significant interaction between time and genotype on serum corticosterone, with a blunting of night/day differences in *AS^{Cre/+};;Bmal1 KO* mice vs. control when the mice were in metabolic cages.

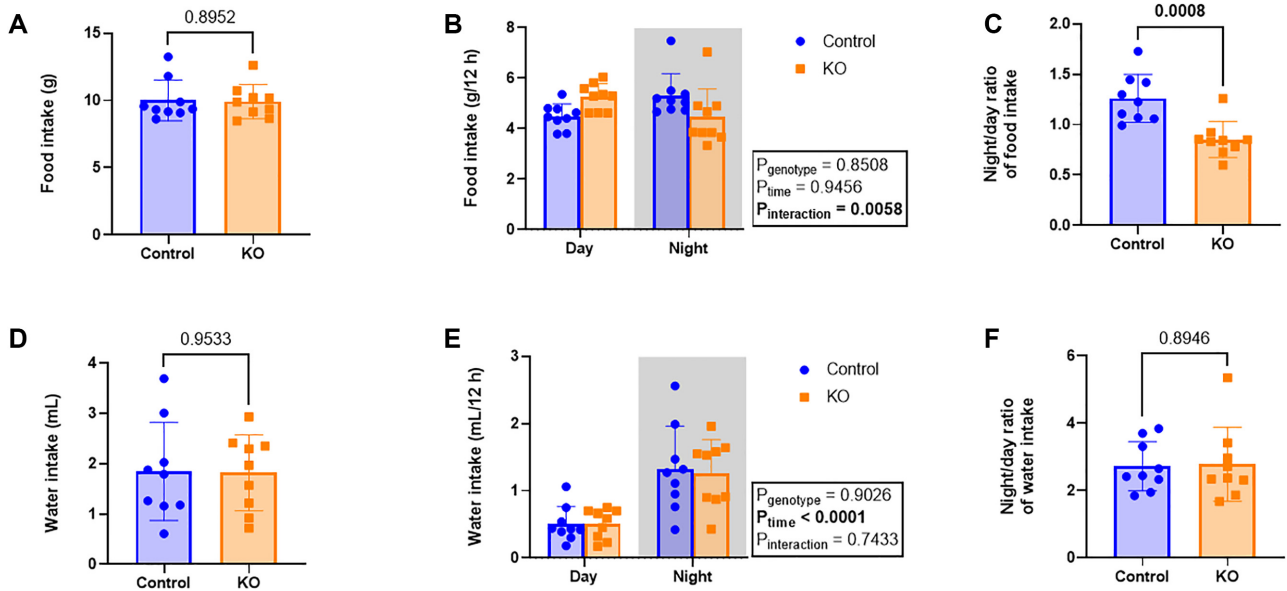


Figure 4. *AS^{Cre/+}::Bmal1* KO mice exhibit blunted night/day differences in food intake, but not water intake in metabolic cages. Twenty-four-hour food (A) and water intake (D), 12-h food (B) and water (E) intake, and night/day ratio of food (C) and water (F) intake in control (blue circles, $n = 9$) and *AS^{Cre/+}::Bmal1* KO (orange squares, $n = 9$) male mice. Values are expressed as means \pm SD. Student's t-test was used to compare genotypes. Genotype, time, and interaction effects were determined by a 2-way ANOVA with repeated measures.

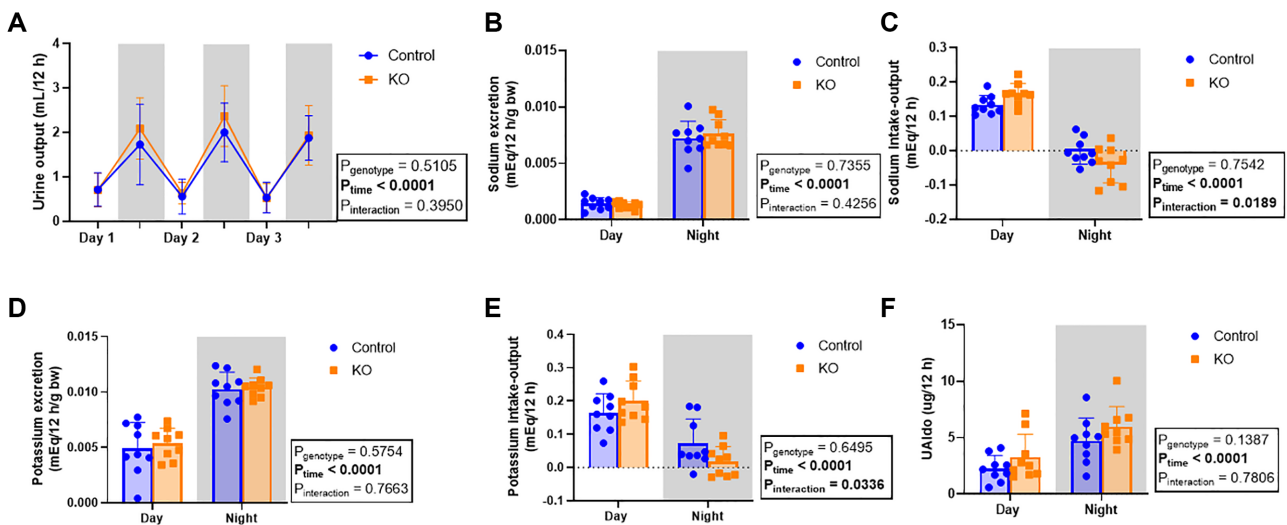


Figure 5. *AS^{Cre/+}::Bmal1* KO mice displayed altered timing of sodium and potassium balance. Urine output over 3 d on the control diet in control (blue circles, $n = 9$) and *AS^{Cre/+}::Bmal1* KO (orange squares, $n = 9$) male mice (A). Twelve-hour (day and night) sodium excretion (B), sodium balance (input-output, C), potassium excretion (D), and potassium balance (E) averaged over the 3-d period. Day and night urinary aldosterone concentration (UAldo) was measured on the final day of the experiment (F). Values are expressed as means \pm SD. Genotype, time, and interaction effects were determined by a 2-way ANOVA with repeated measures.

Discussion

The main findings of this study are that KO of BMAL1 in the zona glomerulosa of the adrenal cortex in male mice results in a shortened BP and activity circadian cycle (period), and delayed peak of BP and activity. Importantly, these results were observed when the mice were housed in metabolic cages, which in our hands acted as a stressor as serum corticosterone was elevated, and *AS^{Cre/+}::Bmal1* KO mice lost the night/day difference in serum corticosterone. Furthermore, these mice showed altered eating behaviors with a blunted night/day ratio of food intake, but overall did not eat anymore compared with controls. Although sodium and potassium excretion were not affected, this effect was associated with changes in the timing of both

sodium and potassium balance. Overall, these data suggest that BMAL1 in the adrenal cortex has a role in the regulation of BP rhythm in response to stress.

Previously, we showed a lower BP phenotype in kidney-specific *Bmal1* KO male mice,²¹ consistent with previous findings in other KO mouse models of BMAL1.^{16,17,19,20,22} However, in the present study, *AS^{Cre/+}::Bmal1* KO male mice did not exhibit a reduction in BP during basal conditions or following placement in metabolic cages, suggesting zona glomerulosa BMAL1 does not play a role in this BP-lowering phenotype or that compensatory mechanisms abrogate its effect. With the global *Bmal1* KO mice displaying blunting of the BP rhythm, the mechanisms behind this are of interest. The BP dip was not altered, showing

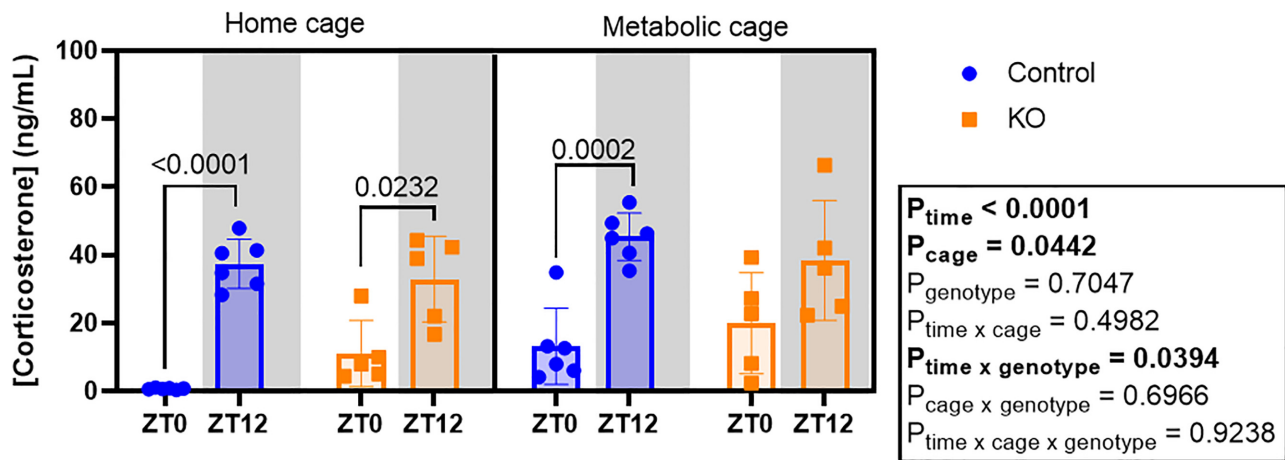


Figure 6. *AS^{Cre/+}::Bmal1* KO mice display blunted night/day differences in serum corticosterone. Serum corticosterone in control (blue circles) and *AS^{Cre/+}::Bmal1* KO (orange squares) male mice at ZT0 (lights on) and ZT12 (lights off) in home cages and metabolic cages. Values are expressed as means \pm SD ($n = 5-6$). Genotype, cage, time, and interaction effects were determined by a 3-way ANOVA with repeated measures (significant post hoc comparisons shown).

a fall in BP during the rest phase in control and *AS^{Cre/+}::Bmal1* KO mice. However, aspects of the BP circadian rhythm were altered, including a shortening of the period and a shift of the acrophase in MAP and activity, which was evident in metabolic cages but not home cages. Rayleigh plot analysis showed that the acrophase of these parameters occurred in a synchronized manner as the data were clustered together, but was delayed in the KO. Both MAP and HR increased in metabolic cages and remained elevated after 5 d in both genotypes. This effect has been shown in mice on a mixed C57BL/6 J/129/sv background, but in these mice, MAP did return to baseline following day 1 in the metabolic cages, with HR remaining elevated.³⁴ HR remained elevated in our study, and there was a significant interaction between time and genotype in the metabolic cages. Cosinor analysis was carried out on this dataset and showed that the robustness of HR (strength of the rhythm) was only $\sim 20\%$ for both genotypes. Robustness below 20% is likely to be biological noise instead of signal.²⁹ Therefore, future work will assess HR variability to further investigate differences in HR over time in *AS^{Cre/+}::Bmal1* KO mice.

There are many key regulators of the 24-h BP profile that could contribute to changes in the length of the period and shift in acrophase including, but not restricted to, ambient temperature, light, food, stress, activity, sleep/wake cycles, the autonomic and central nervous systems, and the renin-angiotensin-aldosterone system (reviewed in³⁵). Ambient temperature and a 12-h light/12-h dark cycle were maintained throughout the experiment. Furthermore, urinary aldosterone was not different between genotypes under steady-state conditions. However, the timing of eating behavior was shifted in *AS^{Cre/+}::Bmal1* KO mice, with a blunting of the night/day ratio of food intake. Food has been shown to be a strong Zeitgeber for peripheral clocks as restricted feeding to the rest phase in mice inverts the phase of circadian clock expression in the kidney, liver, heart, and pancreas,³⁶ which is likely to have influences on physiological functions. In fact, time of feeding has been previously shown to drive the circadian rhythm of BP, as restricted feeding to the rest phase for 6 d inverted the diurnal rhythm of MAP.³⁷ This appeared independent of BMAL1 under basal conditions, as restricted feeding in global *Bmal1* KO male mice also displayed inverted diurnal rhythm of MAP. This restricted feeding interestingly shifted the acrophase of MAP, HR, and activity. In the present study,

the KO animals have altered timing of eating behavior during *ad libitum* feeding, this could be a potential mechanism behind the shifted acrophase of MAP and activity seen in the metabolic cages.

Metabolic cages acted as a stressor in this study, as serum corticosterone was significantly increased compared with mice in their home cages, consistent with previous studies in rodents.^{38,39} Furthermore, prior work found increased response to stress following acute restraint stressor in adrenal-specific *Cyp11A1^{Cre/+}::Bmal1^{Fl/Fl}* KO mice.²⁴ The magnitude of the stressor was significantly higher than when placed in metabolic cages, but nevertheless, the serum corticosterone response was significantly altered following this mild stressor. Interestingly, we see a significant interaction between time and genotype in male *AS^{Cre/+}::Bmal1* KO mice, with a blunting of time-of-day differences in metabolic cages. Corticosterone has been previously measured in male adrenal-specific *Cyp11A1^{Cre/+}::Bmal1^{Fl/Fl}* KO mice, showing no significant differences at baseline.^{24,26} However, only one time point was measured. The altered corticosterone profile in *AS^{Cre/+}::Bmal1* KO male mice could explain the differences seen between genotypes following a mild stressor. Glucocorticoids are increased following a stressor and/or following increased sympathetic nervous system (SNS) tone, to increase mobilization of energy to maintain homeostasis and promote survival. Interestingly, stress-induced increase in SNS tone can impact HR and BP to adapt to the stressor.⁴⁰ Therefore, this could also influence BP and activity rhythm, so future work will look to measure catecholamines in *AS^{Cre/+}::Bmal1* KO mice. Stress has been linked to both increased and decreased food intake, thought to be dependent on stress intensity and/or frequency.⁴¹ Evidence has also shown that glucocorticoids can regulate the timing of eating in rodents.⁴² It is tempting to speculate that this could be a potential mechanism behind altered timing of food intake, which may subsequently influence BP and activity rhythm. Time of eating can also alter the rhythm of glucocorticoid secretion, where 7 d of daytime feeding in mice resulted in a bimodal distribution of serum corticosterone where the first peak occurred at ZT0 with a second peak between ZT8 and 12.⁴³ Therefore, this could create a disruptive cycle between timing of glucocorticoid secretion and eating when challenging *AS^{Cre/+}::Bmal1* KO mice with a stressor, causing changes to BP and activity rhythm.

The initial goal of this study was to place mice in metabolic cages to accurately measure food and water intake and urine output while these mice underwent radiotelemetry measures. However, the metabolic cages acted as a mild stressor, and, interestingly, this is where differences were seen. A limitation of the current study is that this work was only carried out in male mice. With an exaggerated response to stressors previously reported in female *AS^{Cre/+}::Bmal1* KO animals,²⁴ future studies will investigate the role of adrenal BMAL1 in both males and females on feeding behaviors and BP rhythm in response to prolonged and/or more moderate stress. Another limitation is the lack of more temporal resolution in the serum corticosterone data. Future studies will look to assess the response to prolonged and/or more moderate stress with measurements collected every 4 h over a 24-h period.

A question that has arisen from this study is whether the effects of altered time of eating and altered BP and activity rhythms are compensatory or maladaptive? This is of interest as irregular feeding times and disruption of circadian rhythmicity can lead to circadian misalignment, hormonal imbalance, increased HR, sleep disorders, increased BP, and therefore, overall increasing risk of cardiovascular disease.^{44–46} To address these questions, future work will investigate the long-term effects of chronic stress on time of feeding and BP rhythm and how the adrenal circadian clock plays a role in this. Future experiments are likely to include time-restricted feeding, as limiting the time of food intake to the mouse active period has been shown to improve circadian behavior and cardiovascular rhythms.^{47,48}

Notably, this study shows for the first time that KO of BMAL1 specifically in the zona glomerulosa of the adrenal gland results in altered circadian rhythms in BP and activity, blunted night/day ratio of food intake, changes in timing of both sodium and potassium balance, and blunted night/day differences in serum corticosterone in the setting of a metabolic cage. Circadian rhythm defects typically require constant conditions to be revealed.⁴⁹ Thus, these findings are quite remarkable in that they were clearly evident under normal light:dark conditions.

Acknowledgments

The authors wish to thank Dr. Karyn A. Esser for providing the floxed BMAL1 mice and Dr. David Breault for providing the adrenal-specific aldosterone synthase (*AS^{Cre/+}, Cyp11b2^{tm1.1(cre)Brlt}*) Cre recombinase mice.

Funding

This work was supported by the American Heart Association (Postdoctoral Fellowship P0240441 to H.M.C.; Established Investigator Award 19EIA34660135 to M.L.G.), the Robert and Mary Cade Professorship in Physiology (to M.L.G.), and the NIH (F32DK121424 to G.R.C.).

Conflict of Interest

There are no disclosures or conflicts of interest.

Data Availability Statement

The data underlying this article will be shared on reasonable request to the corresponding author.

References

- de la Sierra A, Segura J, Gorostidi M, Banegas JR, de la Cruz JJ, Ruilope LM. Diurnal blood pressure variation, risk categories and antihypertensive treatment. *Hypertens Res* 2010;**33**(8):767–771.
- Zelinski EL, Deibel SH, McDonald RJ. The trouble with circadian clock dysfunction: multiple deleterious effects on the brain and body. *Neurosci Biobehav Rev* 2014;**40**:80–101.
- Costello HM, Gumz ML. Circadian rhythm, clock genes, and hypertension: recent advances in hypertension. *Hypertension* 2021;**78**(5):1185–1196.
- Smith AC. Spring forward at your own risk: daylight saving time and fatal vehicle crashes. *Am Econ J Appl Econ* 2016;**8**(2):65–91.
- Rishi MA, Ahmed O, Barrantes Perez JH, et al. Daylight saving time: an American Academy of Sleep Medicine position statement. *J Clin Sleep Med* 2020;**16**(10):1781–1784.
- Egan BM, Kjeldsen SE, Grassi G, Esler M, Mancia G. The global burden of hypertension exceeds 1.4 billion people. *J Hypertens* 2019;**37**(6):1148–1153.
- Mancia G, Fagard R, Narkiewicz K, et al. 2013 ESH/ESC Guidelines for the management of arterial hypertension: the Task Force for the management of arterial hypertension of the European Society of Hypertension (ESH) and of the European Society of Cardiology (ESC). *J Hypertens* 2013;**31**(7):1281–1357.
- Douma LG, Gumz ML. Circadian clock-mediated regulation of blood pressure. *Free Radical Biol Med* 2018;**119**:108–114.
- Buijs RM, Kalsbeek A. Hypothalamic integration of central and peripheral clocks. *Nat Rev Neurosci* 2001;**2**(7):521–526.
- Refinetti R. Comparison of light, food, and temperature as environmental synchronizers of the circadian rhythm of activity in mice. *J Physiol Sci* 2015;**65**(4):359–366.
- Heyde I, Oster H. Differentiating external zeitgeber impact on peripheral circadian clock resetting. *Sci Rep* 2019;**9**(1):20114.
- Hastings MH, Reddy AB, Maywood ES. A clockwork web: circadian timing in brain and periphery, in health and disease. *Nat Rev Neurosci* 2003;**4**(8):649–661.
- Takahashi JS. Transcriptional architecture of the mammalian circadian clock. *Nat Rev Genet* 2017;**18**(3):164–179.
- Gumz ML. Molecular basis of circadian rhythmicity in renal physiology and pathophysiology. *Exp Physiol* 2016;**101**(8):1025–1029.
- Partch CL, Green CB, Takahashi JS. Molecular architecture of the mammalian circadian clock. *Trends Cell Biol* 2014;**24**(2):90–99.
- Curtis AM, Cheng Y, Kapoor S, Reilly D, Price TS, FitzGerald GA. Circadian variation of blood pressure and the vascular response to asynchronous stress. *Proc Natl Acad Sci* 2007;**104**(9):3450–3455.
- Xie Z, Su W, Liu S, et al. Smooth-muscle BMAL1 participates in blood pressure circadian rhythm regulation. *J Clin Invest* 2015;**125**(1):324–336.
- Coffman TM, Crowley SD. Kidney in hypertension. *Hypertension* 2008;**51**(4):811–816.
- Nikolaeva S, Ansermet C, Centeno G, et al. Nephron-specific deletion of circadian clock gene *Bmal1* alters the plasma and renal metabolome and impairs drug disposition. *J Am Soc Nephrol* 2016;**27**(10):2997–3004.
- Zhang D, Jin C, Obi IE, et al. Loss of circadian gene *Bmal1* in the collecting duct lowers blood pressure in male, but

- not female, mice. *Am J Physiol Renal Physiol* 2020;**318**(3):F710–F719.
21. Crislip GR, Douma LG, Masten SH, et al. Differences in renal BMAL1 contribution to Na⁺ homeostasis and blood pressure control in male and female mice. *Am J Physiol Renal Physiol* 2020;**318**(6):F1463–F1477.
 22. Tokonami N, Mordasini D, Pradervand S, et al. Local renal circadian clocks control fluid–electrolyte homeostasis and BP. *J Am Soc Nephrol* 2014;**25**(7):1430–1439.
 23. Ivy JR, Oosthuyzen W, Peltz TS, et al. Glucocorticoids induce nondipping blood pressure by activating the thiazide-sensitive cotransporter. *Hypertension* 2016;**67**(5):1029–1037.
 24. Engeland WC, Massman L, Miller L, et al. Sex differences in adrenal Bmal1 deletion-induced augmentation of glucocorticoid responses to stress and ACTH in mice. *Endocrinology* 2019;**160**(10):2215–2229.
 25. Freedman BD, Kempna PB, Carlone DL, et al. Adrenocortical zonation results from lineage conversion of differentiated zona glomerulosa cells. *Dev Cell* 2013;**26**(6):666–673.
 26. Engeland WC, Massman L, Mishra S, et al. The adrenal clock prevents aberrant light-induced alterations in circadian glucocorticoid rhythms. *Endocrinology* 2018;**159**(12):3950.
 27. Butz GM, Davissou RL. Long-term telemetric measurement of cardiovascular parameters in awake mice: a physiological genomics tool. *Physiol Genomics* 2001;**5**(2):89–97.
 28. Stow LR, Richards J, Cheng KY, et al. The circadian protein period 1 contributes to blood pressure control and coordinately regulates renal sodium transport genes. *Hypertension* 2012;**59**(6):1151–1156.
 29. Refinetti R, Corné Lissen G, Halberg F. Procedures for numerical analysis of circadian rhythms. *Biol Rhythm Res* 2007;**38**(4):275–325.
 30. Zietara A, Spires DR, Juffre A, et al. Knockout of the circadian clock protein PER1 (Period1) exacerbates hypertension and increases kidney injury in dahl salt-sensitive rats. *Hypertension* 2022;**79**(11):2519–2529.
 31. Douma LG, Costello HM, Crislip GR, et al. Kidney-specific KO of the circadian clock protein PER1 alters renal sodium handling, aldosterone levels, and kidney/adrenal gene expression. *Am J Physiol Renal Physiol* 2022;**322**(4):F449–F459.
 32. Solocinski K, Holzworth M, Wen X, et al. Desoxycorticosterone pivalate-salt treatment leads to non-dipping hypertension in Per1 knockout mice. *Acta Physiologica* 2017;**220**(1):72–82.
 33. Lum C, Shesely EG, Potter DL, Beierwaltes WH. Cardiovascular and renal phenotype in mice with one or two renin genes. *Hypertension* 2004;**43**(1):79–86.
 34. Hoppe CC, Moritz KM, Fitzgerald SM, Bertram JF, Evans RG. Transient hypertension and sustained tachycardia in mice housed individually in metabolism cages. *Physiol Res* 2009;**58**(1):69–75.
 35. Smolensky MH, Hermida RC, Portaluppi F. Circadian mechanisms of 24-hour blood pressure regulation and patterning. *Sleep Med Rev* 2017;**33**:4–16.
 36. Damiola F, le Minh N, Preitner N, Kornmann B, Fleury-Olela F, Schibler U. Restricted feeding uncouples circadian oscillators in peripheral tissues from the central pacemaker in the suprachiasmatic nucleus. *Genes Dev* 2000;**14**(23):2950–2961.
 37. Zhang D, Colson JC, Jin C, et al. Timing of food intake drives the circadian rhythm of blood pressure. *Function (Oxf)* 2021;**2**(1):zqaa034. doi:10.1093/function/zqaa034
 38. Sahin Z, Solak H, Koc A, et al. Long-term metabolic cage housing increases anxiety/depression-related behaviours in adult male rats. *Arch Physiol Biochem* 2019;**125**(2):122–127.
 39. Kallikoski O, Jacobsen KR, Darusman HS, et al. Mice do not habituate to metabolism cage housing—a three week study of male BALB/c mice. *PLoS One* 2013;**8**(3):e58460. doi:10.1371/journal.pone.0058460
 40. Ulrich-Lai YM, Herman JP. Neural regulation of endocrine and autonomic stress responses. *Nat Rev Neurosci* 2009;**10**(6):397–409.
 41. Thompson AK, Fourman S, Packard AEB, Egan AE, Ryan KK, Ulrich-Lai YM. Metabolic consequences of chronic intermittent mild stress exposure. *Physiol Behav* 2015;**150**:24–30.
 42. Tempel DL, Leibowitz SF. Adrenal steroid receptors: interactions with brain neuropeptide systems in relation to nutrient intake and metabolism. *J Neuroendocrinol* 1994;**6**(5):479–501.
 43. le Minh N, Damiola F, Tronche F, Schütz G, Schibler U. Glucocorticoid hormones inhibit food-induced phase-shifting of peripheral circadian oscillators. *EMBO J* 2001;**20**(24):7128–7136.
 44. Walker WH, Walton JC, DeVries AC, Nelson RJ. Circadian rhythm disruption and mental health. *Transl Psychiatry* 2020;**10**(1):28. doi:10.1038/s41398-020-0694-0
 45. Reutrakul S, Knutson KL. Consequences of circadian disruption on cardiometabolic health. *Sleep Med Clin* 2015;**10**(4):455–468.
 46. Morris CJ, Purvis TE, Hu K, Scheer FAJL. Circadian misalignment increases cardiovascular disease risk factors in humans. *Proc Natl Acad Sci* 2016;**113**(10):E1402–11.
 47. Chaix A, Lin T, Le HD, Chang MW, Panda S. Time-restricted feeding prevents obesity and metabolic syndrome in mice lacking a circadian clock. *Cell Metab* 2019;**29**(2):303–319.e4.
 48. Hou T, Su W, Duncan MJ, Olga VA, Guo Z, Gong MC. Time-restricted feeding protects the blood pressure circadian rhythm in diabetic mice. *Proc Natl Acad Sci* 2021;**118**(25):e2015873118. doi:10.1073/pnas.2015873118
 49. Bae K, Jin X, Maywood ES, Hastings MH, Reppert SM, Weaver DR. Differential functions of mPer1, mPer2, and mPer3 in the SCN circadian clock. *Neuron* 2001;**30**(2):525–536.